New Technologies in Ophthalmology

Ophthalmologica

Ophthalmologica
DOI: 10.1159/000502458

Received: April 9, 2019
Accepted after revision: July 31, 2019
Published online: September 11, 2019

OCT Angiography: Measurement of Retinal Macular Microvasculature with Spectralis II OCT Angiography – Reliability and Reproducibility

Sami Hosari[a] Bettina Hohberger[a] Luisa Theelke[b] Hasan Sari[c]
Marianna Lucio[d] Christian Y. Mardin[a]

[a]Department of Ophthalmology, Friedrich-Alexander University of Erlangen-Nürnberg, Erlangen, Germany; [b]Department of Computer Science 5, Friedrich-Alexander University of Erlangen-Nürnberg, Erlangen, Germany; [c]Department of Clinical Neurosciences, University of Cambridge, Cambridge, UK; [d]Research Unit Analytical Biogeochemistry, German Research Center for Environmental Health, Helmholtz Zentrum München, Neuherberg, Germany

Keywords
Optical coherence tomography angiography · Retina · Macula · Microvasculature · Measurement · Foveal avascular zone

Abstract
Aim: The aim of the present study was to investigate the reliability of macular microvasculature measurements in normal subjects by Heidelberg Spectralis II optical coherence tomography angiography (OCT-A) in combination with a newly made software. ***Subjects and Methods:*** This prospective study included 23 eyes of 23 persons from the Erlangen Glaucoma Registry (ISSN 2191–5008, CS-2011; NTC00494923). The subjects underwent a complete clinical, standardized ophthalmologic examination to rule out any eye disease. En face OCT-A imaging was done using Heidelberg Spectralis II OCT (Heidelberg, Germany). Images were recorded with a 15 × 15° angle and a lateral resolution of 5.7 µm/pixel, resulting in a retinal section of 2.9 × 2.9 mm. The Erlangen-Angio-Tool (EA-Tool) OCT-A application performed multiple segmentations, allowing analysis of the vessel density in 12 segments. The software was coded in MATLAB. Macular data on the superficial vascular plexus (SVP), intermediate capillary plexus (ICP), and deep capillary plexus (DCP) were exported into the application and analyzed separately. The EA-Tool calculated the percentage of "white area" in the "total area" of the region of interest, called vessel density. Foveolar avascular zones (FAZs) of the SVP, ICP, and DCP were calculated manually. To investigate the reproducibility of the new software, individual scans (SVP, ICP, and DCP) were analyzed twice with the EA-Tool and intraclass coefficients (ICCs) of the vessel density values were calculated. Statistical analysis was performed with SPSS version 21.0. ***Results:*** The mean vessel density of the SVP ranged between 30.4 and 33.5, that of the ICP between 20.9 and 24.7, and that of the DCP between 23.5 and 27.6. Bland-Altman plots showed a good reliability of two consecutive scans of each sector (S1–S12) in the SVP, ICP, and DCP. Testing reproducibility, no statistically significantly different sectorial coefficients of variation of the SVP, ICP, and DCP were observed ($p > 0.05$). The mean FAZ area of the SVP was 0.43 ± 0.16 mm^2, that of the ICP 0.28 ± 0.1 mm^2, and that of the DCP 0.44 ± 0.12 mm^2. ***Conclusions:*** Spectralis OCT II, in combination with the semiautomated vessel density soft-

The present work was carried out in (partial) fulfillment of the requirements for obtaining the degree "Dr. med." (S.H.).

E-Mail karger@karger.com
www.karger.com/oph

Prof. Christian Y. Mardin
Department of Ophthalmology
Friedrich-Alexander University of Erlangen-Nürnberg
Schwabachanlage 6, DE–91054 Erlangen (Germany)
E-Mail christian.mardin@uk-erlangen.de

ware EA-Tool, showed good or even excellent ICCs in 75% of all segments of the SVP, ICP, and DCP. The ICCs for the FAZ area in the SVP, ICP, and DCP were excellent.

Introduction

Analysis of the retinochoroidal microvasculature is an important diagnostic tool for clinical everyday life and research issues. Visualization of the vessels' structure and their perfusion can be done by invasive techniques (e.g., fluorescence angiography); yet, a recent noninvasive technique was introduced by Makita et al. [1] and Jia et al. [2]. Optical coherence tomography angiography (OCT-A) enables fast and noninvasive 3D imaging of the retinochoroidal vasculature with high spatial resolution. Using a motion contrast algorithm, dye injection is not necessary to visualize vessels of the retina and choroid. OCT-A of the first generation showed the microvasculature of two distinct retinal vascular layers: the superficial vascular plexus (SVP) and the deep capillary plexus (DCP) [3]. The latest version of the Spectralis II implements visualization of a third vascular layer, the intermediate capillary plexus (ICP), localized between the SVP and DCP [4]. These three microvascular layers were seen to correlate well with anatomical structures [5].

Several different OCT-A tools are currently available; however, each manufacturer uses its own algorithm for generating vascular images based on OCT signal information (e.g., a full-spectrum amplitude algorithm or a split-spectrum amplitude algorithm) [6, 7]. Additionally, different software tools and algorithms with consecutively different binarization were used for the evaluation of OCT-A images [3, 6, 8, 9]. Due to these facts, different vessel density values were observed when using OCT-A systems of diverse manufacturers. Thus, it is important to investigate the reliability of each OCT-A device and analysis software. Only one reliability study is currently available, using Heidelberg Spectralis II OCT-A and custom-made software (AngiOCTool version 4.0), analyzing foveal avascular zone (FAZ) metrics as well as SVP and DCP vessel density. At present there is no commercially available evaluation software to use Spectralis II OCT-A images.

The aim of the present study was to investigate the reliability of macular microvasculature measurements in normal subjects by Heidelberg Spectralis II OCT-A in combination with a newly made MATLAB (The MathWorks, Inc.; R2017b) software (Erlangen-Angio-Tool [EA-Tool] version 1.0). Intraclass correlation coefficients (ICCs) of vessel density and FAZ for the SVP, ICP, and DCP were calculated.

Subjects and Methods

Participants

The present, prospective study included 23 eyes of 23 persons from the Erlangen Glaucoma Registry (ISSN 2191-5008, CS-2011; NTC00494923) of the Department of Ophthalmology, Friedrich-Alexander University Erlangen-Nürnberg, Germany. All subjects underwent a complete standardized ophthalmologic examination including slit-lamp biomicroscopy, funduscopy, and Goldmann applanation tonometry. White-on-white perimetry (Octopus 500, program G1; Interzeag AG, Schlieren, Switzerland) was done. The presence of any eye disease was an exclusion criterion. Best corrected visual acuity was ≥0.8. No eye was amblyopic.

OCT Angiography

En face OCT-A imaging was done using Heidelberg Spectralis II OCT (Heidelberg, Germany). The images were recorded with a 15 × 15° angle and a lateral resolution of 5.7 μm/pixel, resulting in a retinal section of 2.9 × 2.9 mm. One of the eyes of each subject was chosen randomly for the en face OCT-A measurements. Two scans were performed within 1 day by the same investigator. Macular data on the SVP (thickness: 80 μm), ICP (thickness: 50 μm), and DCP (thickness: 40 μm) were obtained and exported. The scans were checked for artifacts or shadows prior to analysis.

OCT-A Vessel Density and FAZ Measurements

The EA-Tool OCT-A application performed multiple segmentations, allowing analysis of vessel density. The software was coded in MATLAB. It is designed as stand-alone software with a graphical user interface to work independently from the device. Macular data on the SVP, ICP, and DCP were exported into the application and analyzed separately.

First, a binary picture was generated, in which each vessel pixel (i.e., a pixel belonging to a vessel) was white and each tissue pixel (i.e., a pixel belonging to tissue) was black. For definition of a "vessel pixel," the original image was convolved with a Frangi vesselness filter, based on eigenvalue analysis of the multiscale Hessian image filter response [7, 10]. The resulting image was binarized using the Otsu thresholding algorithm [11] (Fig. 1).

After segmentation, the center of the macular region, being the center of the circle which is defined as the region of interest (ROI), was marked by the user. Therefore, the center of the macula was marked by a geometrical grid and manually approved with a crosshair defining 4 equal quadrants of the FAZ in the en face OCT-A images. The ROI was defined as an annulus, which itself was subdivided into 11 sectors (S1–S12) of 30° each (Fig. 2). In the present study, the inner ring of this annulus had a diameter of 0.80 mm and the outer ring had a diameter of 2.9 mm, resulting in a total ROI area of 6.1 mm^2. The quantification part of the EA-Tool calculated the percentage of "white area" in the "total area" of the ROI, called vessel density. Additionally, the FAZs of the SVP, ICP, and DCP were calculated manually by the same reader by interconnecting the most inward-reaching vessel tails. Afterwards, the application software automatically calculated the total size of the

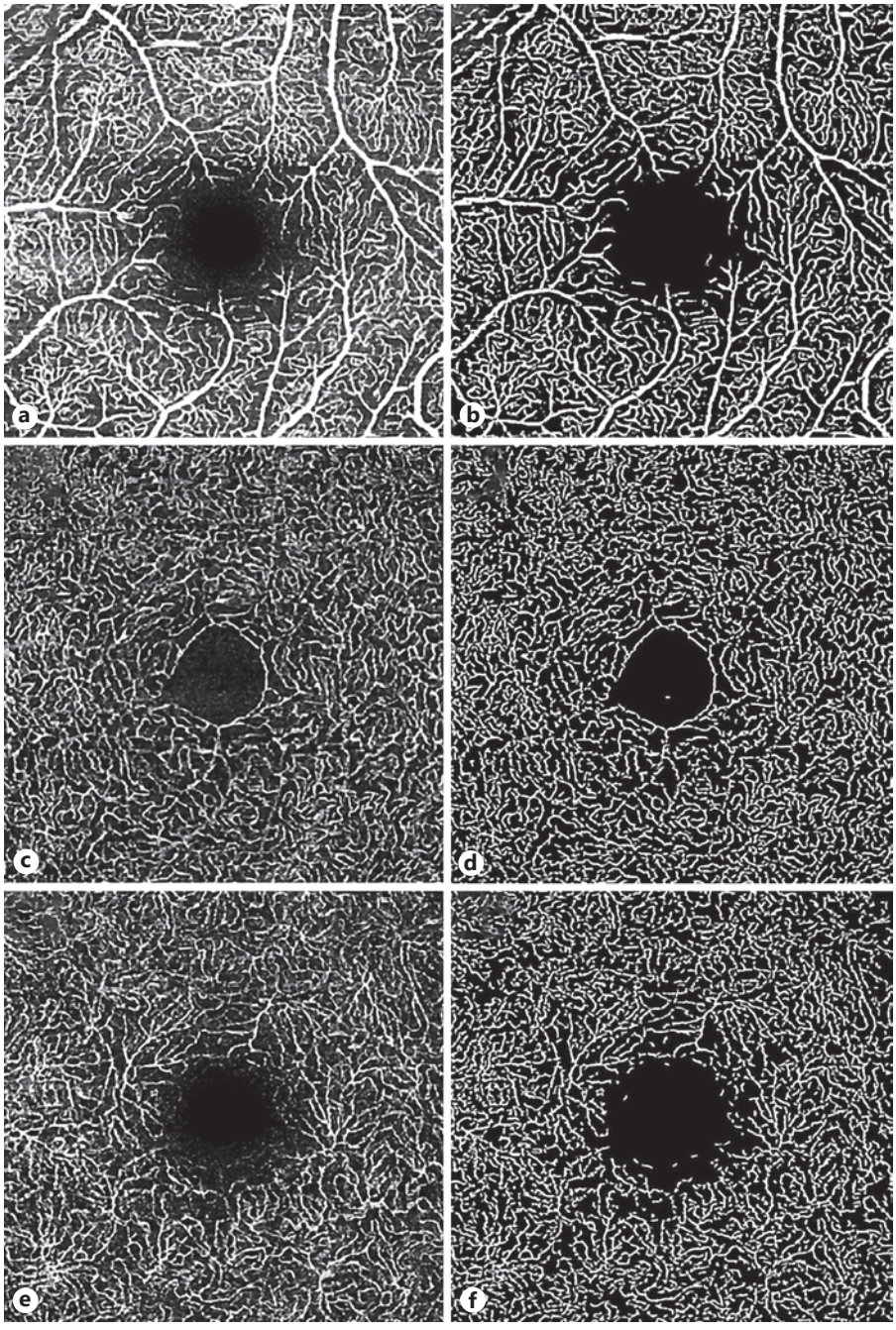

Fig. 1. Optical coherence tomography angiography scans of the superficial vascular plexus (**a**, **b**), intermediate capillary plexus (**c**, **d**), and deep capillary plexus (**e**, **f**) before (**a**, **c**, **e**) and after filtering and thresholding with the EA-Tool (**b**, **d**, **f**).

FAZ within the defined layer. To investigate the reproducibility of our software, we also evaluated one scan (SVP, ICP, DCP) from each subject twice with our EA-Tool and calculated the ICCs of the vessel density values.

Statistics

Statistical analysis was performed with SPSS version 21.0. Demographic and OCT-A data are presented as the mean ± SD. As the SD increased with the magnitude of the measurements, coefficients of variation (CVs) were calculated for the SVP, ICP, DCP, and area of FAZ in order to investigate the reliability of the first and second OCT-A scans; *t* tests, nonparametric tests, and one-way ANOVA were performed for statistical analysis. Bland-Altman plots [12] are presented. Additionally, the power of one-way ANOVA for balanced data was calculated. The input values were the number of observations in each group, their average values, and the estimate SD. We tested if there were differences between the two cases at the 0.05 significance level. The power analysis was conducted with SAS version 9.3 (SAS Institute Inc., Cary, NC, USA).

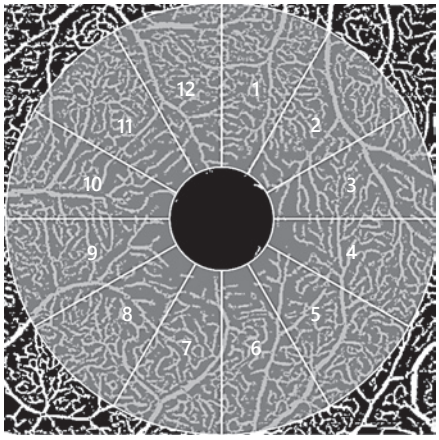

Fig. 2. Region of interest (i.e., macula) marked with an annulus, subdivided into 12 sectors of 30° (S1–S12).

Results

Demographic Data on the Study Population

Twenty-three eyes of 23 normal subjects (14 male and 9 female probands) were included in the present study. The spherical equivalent showed a mean of –0.69 ± 1.4 D. The mean age was 26.8 ± 6 years, with a range of 19–48 years (women: 24.4 ± 5; men: 28.4 ± 7). None of the participants had an ophthalmic disorder. No previous ophthalmic surgery or laser treatment had been performed. The OCT scans showed healthy foveal areas. The intraocular pressure was within the normal range.

Reliability and Reproducibility of Vessel Density Measurements in the SVP, ICP, and DCP

The mean vessel density values of S1–S12 for the SVP, ICP, and DCP on the first scan and the second scan can be seen in Table 1. Additionally, the absolute difference between the first and the second scan is presented. The mean vessel density of the SVP ranged between 30.4 (S10) and 33.5 (S12) on the first scan and between 30.2 (S10) and 33.1 (S12) on the second scan. The ICP showed a lower mean vessel density than the SVP, ranging from 20.9 (S7) to 24.7 (S4) on the first scan and from 21.2 (S7) to 24.9 (S3 and S4) on the second scan. The mean vessel density of the DCP ranged between 23.5 (S8) and 27.6 (S4) on the first scan. The second scan of the DCP showed a mean vessel density between 23.6 (S8) and 27.6 (S4). No statistically significant differences in the vessel densities of S1–S12 between the first and the second scan were observed for the SVP, ICP, and DCP, respectively ($p > 0.05$).

The CVs of the SVP, ICP, and DCP can be seen in Table 1. No statistically significant difference was observed between CVs of the first and the second run for the SVP, ICP, and DCP ($p > 0.05$). Bland-Altman plots represent the good reliability of the two scans of each sector (S1–S12) in the SVP, ICP, and DCP (Fig. 3). Testing reproducibility, no statistically significantly different sectorial CVs of the SVP, ICP, and DCP were observed ($p > 0.05$). The CVs of each sectorial analysis can be seen in Table 2 for each vascular layer.

A subgroup analysis considering myopia (defined as a spherical equivalent >–1.0 D) yielded no statistically significant difference in the CVs of the SVP, ICP, and DCP, respectively ($p > 0.05$). Additionally, no statistically significant differences were observed between the gradings of the two different readers of the vessel densities of the SVP, ICP, and DCP ($p > 0.05$).

Reliability of FAZ Measurements

The mean areas of the FAZ on the first and the second scan can be seen in Table 3. No statistically significant difference was observed between the repeated scans of the FAZ in the SVP, ICP, and DCP, respectively ($p > 0.05$).

The CVs of the first and the second OCT-A run did not differ significantly ($p > 0.05$; Table 3). Additionally, good consistency of the first and the second scan can be seen in the Bland-Altman plots of the SVP, ICP, and DCP (Fig. 4). No statistically significant inter-reader differences were observed for the FAZ of the SVP, ICP, and DCP, respectively ($p > 0.05$).

Power Analysis

An average power of 6% (ICP), 5% (SVP), and 5% (DCP) was observed, respectively. The FAZ yielded an average power of 5% (SVP), 6% (ICP), and 6% (DCP). This means that we had a 5–6% chance to retrieve a statistically significant difference (a p value <0.05) between the two measurements.

Discussion

OCT-A, a technical extension of OCT, is a noninvasive imaging technique based on the motion contrast of moving blood cells' signal amplitude between two repeated scans of the same retinal region. As a new essential part of morphological diagnostics, this technique enables novel diagnostic possibilities and insights into the chorioretinal vasculature. En face OCT-A scans with Spectralis II OCT allow visualization of the vasculature in all retinal layers. This technique, in combination with the semiautomated vessel density software EA-Tool, showed

Table 1. Mean vessel density and CV of the first and the second scan, as well as the AD, of the superficial vascular plexus, intermediate capillary plexus, and deep capillary plexus of all probands, subdivided into 12 sectors (S1–S12)

	Vessel density				AD
	scan 1		scan 2		mean ± SD
	mean ± SD (min.–max.)	CV	mean ± SD (min.–max.)	CV	
Superficial vascular plexus					
S1	32.8±3.2 (24.9–37.7)	16.7	32.7±3.5 (20.7–36.9)	16.8	0.5±0.6
S2	32.6±3.1 (25.1–38.8)	16.2	32.9±2.8 (24.5–37.4)	16.2	0.6±0.5
S3	32.4±2.8 (23.4–36.1)	11.1	32.7±1.9 (26.8–36)	11.5	0.7±0.7
S4	32.9±2.4 (27.4–36.7)	19.1	33.2±2.5 (26.5–37.2)	19.2	0.4±0.5
S5	32.7±3.6 (20.8–36.7)	16.8	33±2.3 (26–35.5)	16.6	0.5±0.4
S6	32.8±4.3 (18.8–37.6)	18.1	33.3±2.8 (25.2–37.6)	18.7	0.1±0.3
S7	32.5±4.3 (20.4–37.8)	20.2	32.4±4.5 (18.3–37)	20.7	0.4±0.3
S8	31.9±4.2 (22–36.8)	22.7	32.2±3.5 (20.5–37.3)	22.4	0.7±0.7
S9	30.6±4.6 (15.8–35.7)	20.0	31.1±3.7 (17.8–36.1)	20.2	0.1±0
S10	30.4±3.2 (23.9–34.1)	19.9	30.2±3.2 (24.6–35.5)	19.8	0±0.1
S11	32.4±2.1 (27.3–35.1)	13.5	32.1±3.1 (23.6–35.5)	13.9	0.2±0.2
S12	33.5±3 (26.9–38.3)	15.0	33.1±4.1 (22.2–38.9)	15.2	0.5±0.5
Intermediate capillary plexus					
S1	23±2.9 (17.9–28.1)	12.3	23±3.1 (15.6–28.2)	12.6	0.1±0.2
S2	23.1±3 (16.2–27.3)	12.9	23.2±2.5 (16.7–26.7)	13.0	0.4±0.5
S3	24.5±3.3 (16.1–30.5)	13.3	24.9±2.5 (17.1–29.2)	13.1	0.2±0.2
S4	24.7±2.8 (18.1–30.6)	16.5	24.9±2.9 (15.9–29.5)	17.0	0.3±0.2
S5	22.5±3.5 (12.2–30.2)	15.4	22.7±3.1 (14.5–28.7)	15.6	0.3±0.1
S6	21.1±4.5 (8.1–29.6)	17.6	21.3±3.2 (15.6–27.1)	18.1	0.3±0.1
S7	20.9±3.8 (11.9–27.2)	19.9	21.2±3.6 (12.7–26.5)	20.0	0.4±0.3
S8	21.4±4.2 (12.4–26.1)	19.7	21.7±3.4 (15–26.7)	19.9	0.3±0.3
S9	22.8±4 (10.6–29.2)	13.0	23.1±3.3 (14.4–28)	12.8	0.3±0.4
S10	23.6±3.3 (13.7–28.5)	14.5	23.3±3.3 (14.6–27.8)	14.2	0.2±0.3
S11	23.1±2.8 (16.5–27.3)	12.3	22.9±3 (16.5–27.6)	12.7	0.3±0.2
S12	23±2.8 (18.5–28)	12.9	22.7±3.5 (13.3–27.6)	13.6	0.4±0.5
Deep capillary plexus					
S1	25.8±3.2 (17.9–33.3)	13.2	25.9±3.4 (16.7–31.5)	13.0	0.1±0.2
S2	25.5±3.5 (15.7–31.7)	12.7	26.2±2.7 (20.8–33.9)	12.6	0.7±0.8
S3	27.3±3.8 (16–32)	12.2	27.5±2.6 (21.2–32.7)	11.8	0.2±0.1
S4	27.6±3 (18.2–31.5)	17.8	27.6±2.9 (19.2–32)	17.6	0.1±0.1
S5	25.4±4 (9.4–29.5)	14.6	25.5±3.4 (17.8–30.7)	15.1	0.1±0
S6	24.8±4.6 (8.4–29.6)	17.3	24.7±4.1 (17.1–31.3)	17.8	0.2±0.4
S7	24.1±4.4 (12.8–30.5)	21.3	24.1±4.6 (12.6–32.6)	21.6	0±0.3
S8	23.5±4.9 (10.4–30)	21.1	23.6±3.6 (15.8–28.3)	21.1	0.1±0.1
S9	24.4±5.1 (8.4–29.8)	15.2	24.9±3.3 (17.3–30)	15.5	0.5±0.5
S10	24.9±3.2 (15.7–29.2)	14.2	24.9±2.9 (16.5–28.9)	14.3	0±0.1
S11	25.3±2.9 (17.3–30.9)	13.2	25.2±2.8 (19.3–30.8)	13.3	0.1±0.1
S12	26.1±3.5 (17.2–33.7)	13.5	26.0±3.8 (15.2–32.6)	14.1	0.1±0.1

AD, absolute difference between the first and the second scan; CV, coefficient of variation.

good or even excellent ICCs in 75% of all segments of the SVP, ICP, and DCP, respectively. Additionally, the ICCs for the FAZ area in the SVP, ICP, and DCP were excellent.

Spectralis II OCT employs a probabilistic full-spectrum amplitude decorrelation algorithm (FSADA). The FSADA scales the signal-to-noise ratio down in favor of a higher axial resolution [2]. In contrast, the split-spectrum amplitude decorrelation algorithm emphasizes noise reduction and imaging of smaller vascular entities, but the axial resolution is lower. This antidromic paradigm of signal to noise leads to different data with each

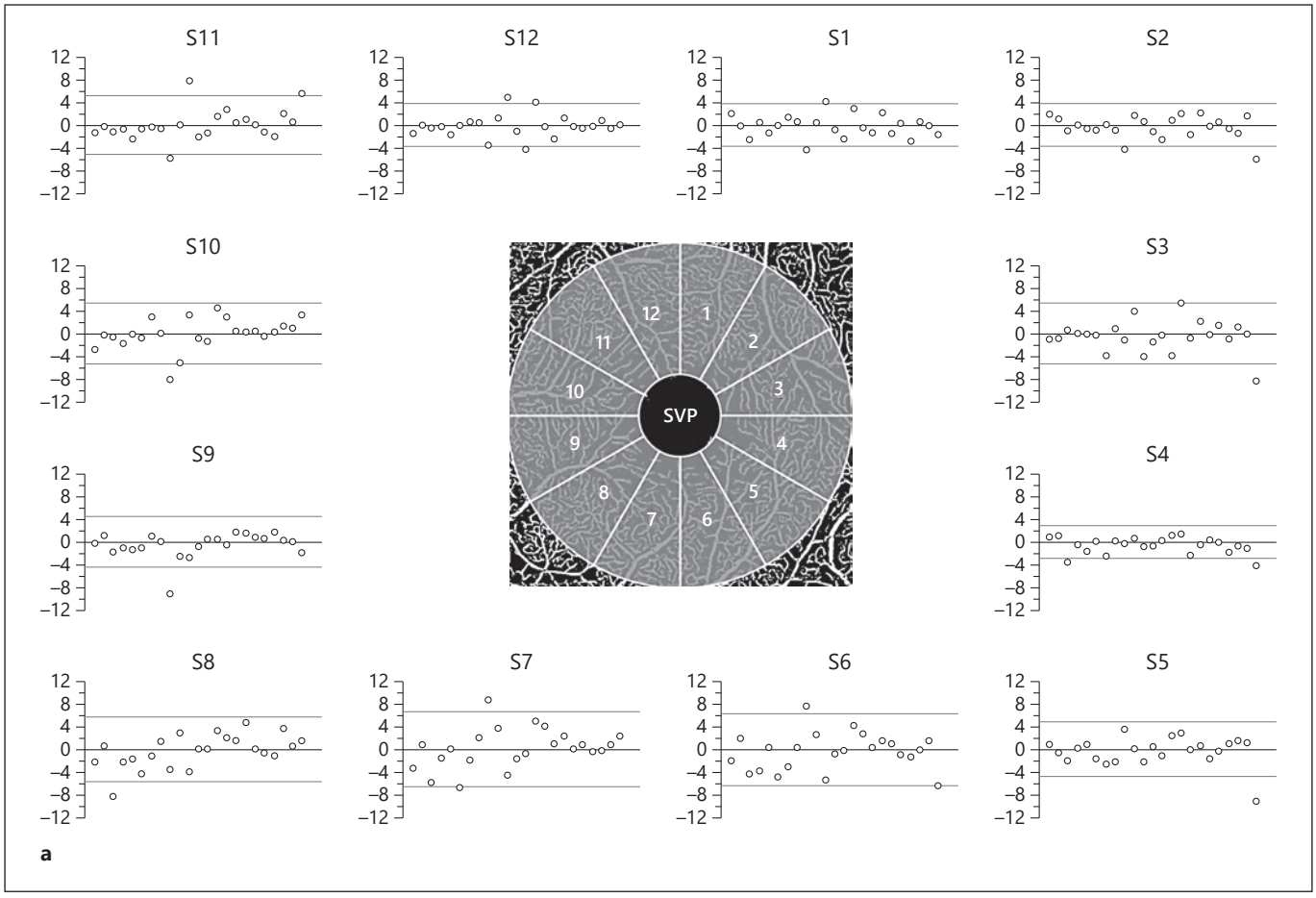

Fig. 3. Bland-Altman plots of the first and the second scan of each sector (S1–S12) of the superficial vascular plexus (SVP; **a**), intermediate capillary plexus (ICP; **b**), and deep capillary plexus (DCP; **c**).

(Figure continued on next pages.)

algorithm. Using the FSADA, Spectralis II OCT shows an axial resolution of 3.9 μm/pixel, enabling precise separation of the distinct vascular layers without projection artifacts in the underlying retinochoroidal layers. The intriguing resolution of OCT-A imaging correlates well with the histological pattern. This fact allows precise in vivo analysis of the retinochoroidal vasculature. Up to now, several studies have investigated vascular alterations in disease (e.g., glaucoma, diabetic retinopathy, and age-related macular degeneration) [13–20]. However, it is important to know the "normal" physiology and anatomy in healthy subjects, as well as the reliability of the methods (i.e., en face OCT-A and analysis software), before transferring the technique to pathophysiological alterations.

Currently, there is only 1 study that investigated the reliability of measurement of two macular vascular layers (the SVP and the DCP) and FAZ characteristics of Spectralis II OCT-A with a custom-made analysis software. Lupidi et al. [8] reported a mean vessel density of 27.84 ± 1.93 (present study: 32.28 ± 3) for the SVP and 27.69 ± 2.23 (present study: 25.40 ± 3.0) for the DCP. No data on the mean vessel density were provided for the ICP. The FAZ areas of the two layers in the previous study were 0.28 ± 0.11 mm^2 (SVP) and 0.30 ± 0.10 mm^2 (DCP), differing from our values (0.43 ± 0.16 mm^2 [SVP], 0.28 ± 0.1 mm^2 [ICP], and 0.44 ± 0.12 mm^2 [DCP]). These discrepancies might be due to different implemented analysis algorithms and software updates like projection artifact removal (PAR). Additionally, Lupidi et al. [8] calculated coefficients of repeatability and reproducibility to demonstrate the reliability of their method; thus, a direct comparison is not possible. The latest software version of Spectralis II uses the PAR tool, eliminating blood movement artifacts from overlying layers. This PAR tool enables an even more distinct look

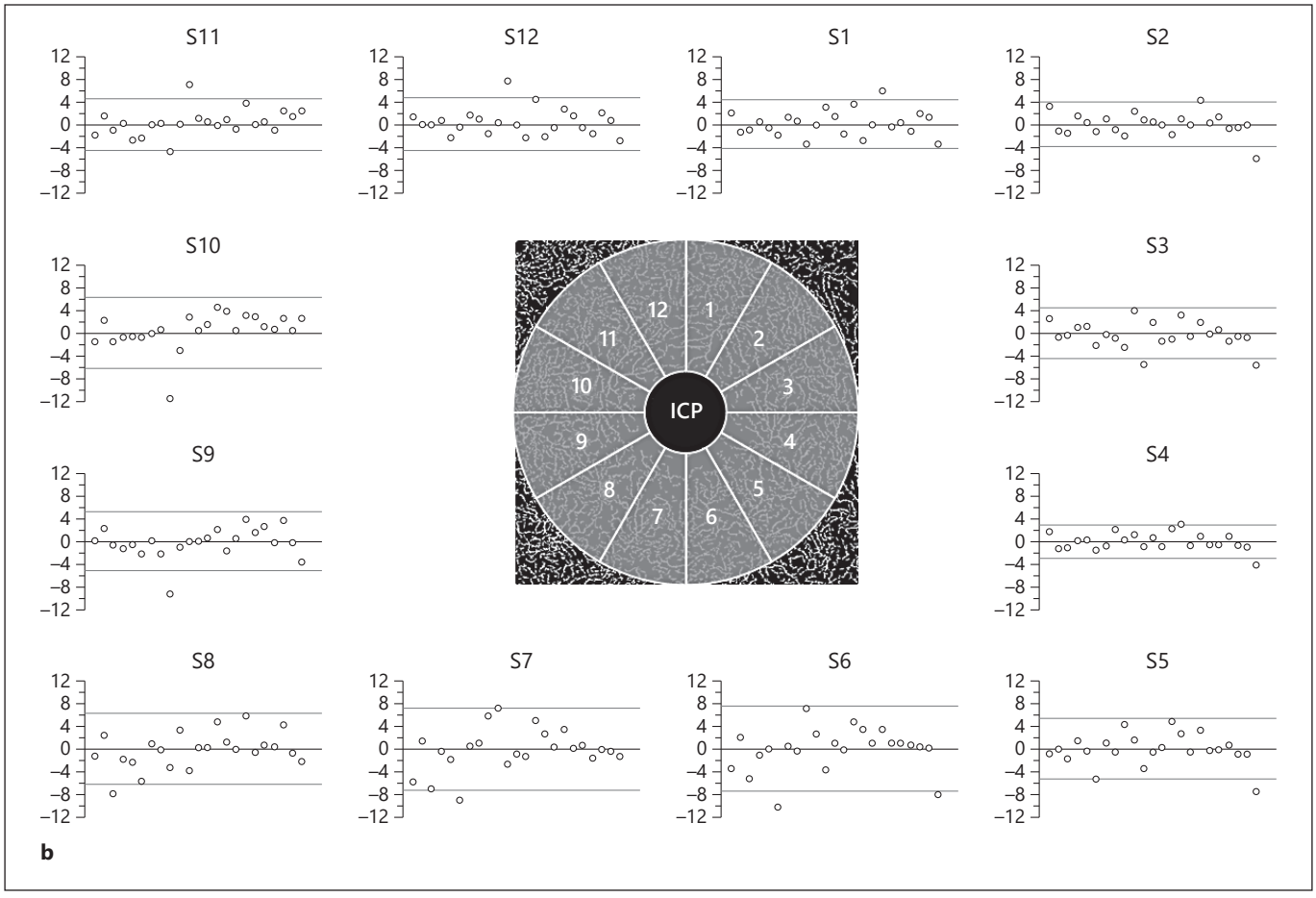

3

at deeper layers (e.g., the ICP and DCP) [21]. Additionally, the TruTrack Active Eye Tracking technology, tracking eye movements and attenuating movement-based artifacts, allows for high-quality retinal imaging even with eye movements. Further evidence for the different data between the two studies might be seen in the ROI, which was larger in our study (i.e., macula, 6.10 mm^2) than in the study by Lupidi et al. [8] (2.86 mm^2), and we had a more detailed B-scan thickness (5.7 vs. 11 μm).

Furthermore, the semiautomated vessel density software EA-Tool uses custom-built filters, improving the quality of each scan and reducing noise (Fig. 1). In a first step, the images were convolved with Frangi's vesselness filter, an image processing technique originally developed for angiogram segmentation. It calculates vesselness features for each pixel based on the eigenvalues of the Hessian matrix with consecutive enhancement of the vessel structures of the image. Additionally, it is relatively insensitive to background noise [10]. Therefore, it can improve subsequent binarization. In order to binarize the images, the Otsu thresholding algorithm was used. This algorithm calculates the optimum threshold based on a statistical analysis of a bimodal histogram. It assumes that the image contains two classes: background and foreground pixels (in our case, tissue pixels and vessel pixels) [11]. This leads to a reliable and comparable binary picture, which then undergoes further calculations (e.g., FAZ measurements and vessel density).

Lupidi et al. [8] calculated coefficients of repeatability and reproducibility to demonstrate the reliability of their method. Our study, in contrast, used ICCs, which also showed excellent results.

Quantification of en face OCT-A images is important in everyday clinical life and for research issues. Even small pathological alterations of the retinal vasculature can have a strong influence on patients' vision. Implementation of the EA-Tool yielded a high spatial resolution of vessel density and FAZ characteristics of the three main vascular layers of the macula.

Our study is not without limitations. The proband group was not very large and their mean age was young

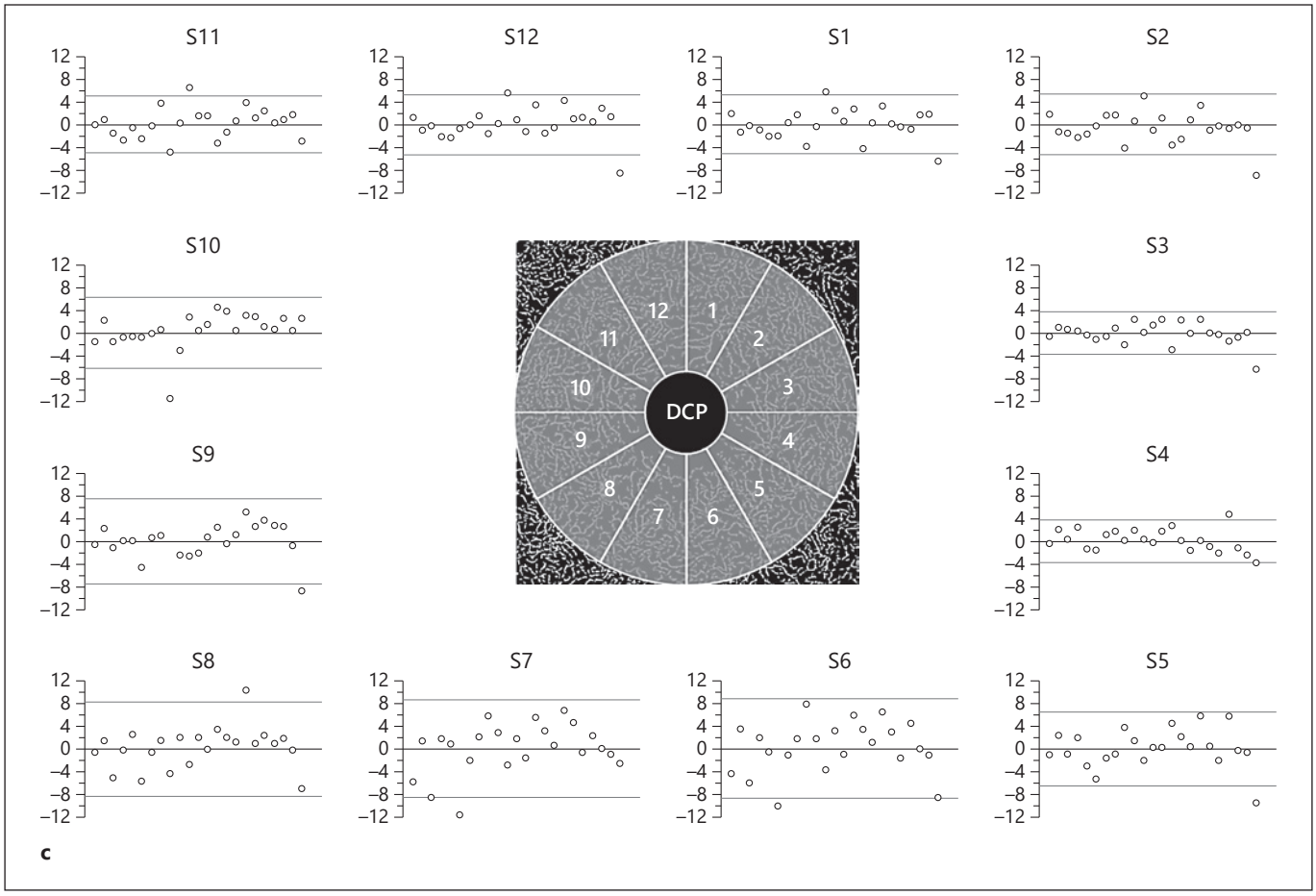

Table 2. Reproducibility of vessel density measurements of one scan evaluated two times: coefficient of variation of the first and the second evaluation of all vessel density values for the three vascular layers

Sector	SVP		ICP		DCP	
	1st evaluation	2nd evaluation	1st evaluation	2nd evaluation	1st evaluation	2nd evaluation
S1	16.7	16.8	12.3	12.6	13.2	13.0
S2	16.2	16.2	12.9	13.0	12.7	12.6
S3	11.1	11.5	13.3	13.1	12.2	11.8
S4	19.1	19.2	16.5	17.0	17.8	17.6
S5	16.8	16.6	15.4	15.6	14.6	15.1
S6	18.1	18.7	17.6	18.1	17.3	17.8
S7	20.2	20.7	19.9	20.2	21.3	21.6
S8	22.7	22.4	19.7	19.9	21.1	21.1
S9	20.0	20.2	13.0	12.8	15.2	15.5
S10	19.9	19.8	14.5	14.2	14.2	14.3
S11	13.5	13.9	12.3	12.7	13.2	13.3
S12	15.0	15.2	12.9	13.6	13.5	14.1

SVP, superficial vascular plexus; ICP, intermediate capillary plexus; DCP, deep capillary plexus.

Table 3. Foveal avascular zone size and CV of the first and the second scan, as well as AD, of all probands for the three vascular layers

	Foveal avascular zone				AD
	scan 1		scan 2		mean ± SD
	mean ± SD (min.–max.)	CV	mean ± SD (min.–max.)	CV	
SVP	0.42±0.23 (0.19–0.8)	38.5	0.43±0.19 (0.21–0.84)	41.3	0.02±0.02
ICP	0.28±0.1 (0.1–0.5)	37.0	0.27±0.11 (0.08–0.5)	38.1	0.01±0.01
DCP	0.44±0.12 (0.22–0.66)	27.9	0.43±0.12 (0.22–0.68)	27.9	0.05±0.04

AD, absolute difference between the first and the second scan; CV, coefficient of variation; SVP, superficial vascular plexus; ICP, intermediate capillary plexus; DCP, deep capillary plexus.

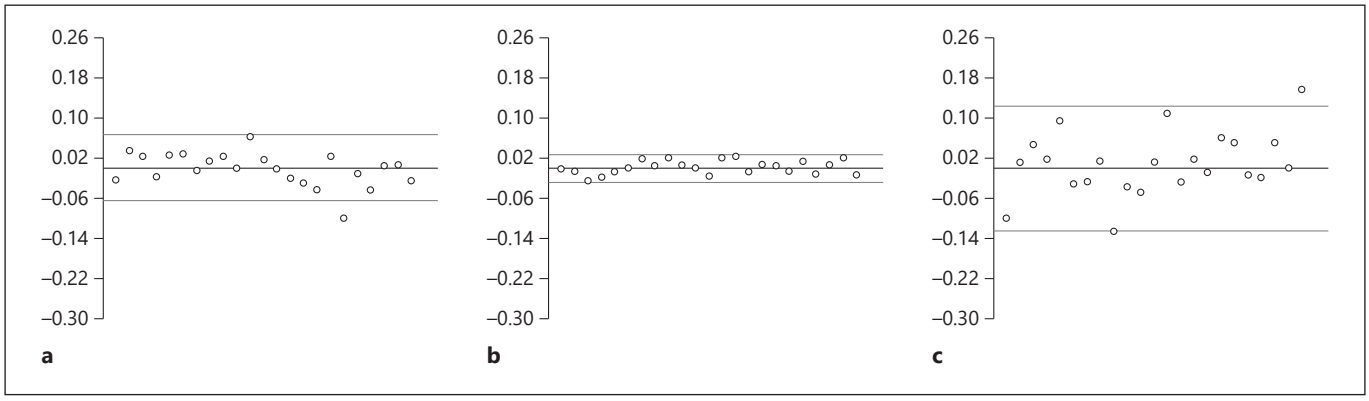

Fig. 4. Bland-Altman plots of the first and the second scan of the foveal avascular zone in the superficial vascular plexus (**a**), intermediate capillary plexus (**b**), and deep capillary plexus (**c**).

at a mean of 26.8 ± 6 years. Thus, all probands had good fixation as a basis for the OCT-A measurements. Yet, scanning the macular or papillary microcirculation might be more difficult in elderly or even diseased people. The data from the present study cannot be seen as "general" normal values for OCT-A measurements. Additionally, studies are necessary to investigate any effects of age on retinal microcirculation in the SVP, ICP, and DCP. Adjuvant studies might investigate inter-visit reliability of Spectralis II OCT-A and EA-Tool measurements considering the circadian rhythm.

Conclusions

The reliability of measurements with en face Spectralis II OCT-A in combination with the EA-Tool software was good or even excellent with regard to intra-visit analysis of SVP, ICP, and DCP as well as FAZ characteristics. The EA-Tool can be used as analysis software for subsequent study of the healthy or diseased macular vasculature for clinical use or research purposes.

Statement of Ethics

The study protocol was approved by the local ethics committee and was performed in accordance with the tenets of the Declaration of Helsinki. Informed consent was obtained from all participating subjects.

Disclosure Statement

All authors certify that they have no affiliations with or involvement in any organization or entity with any financial interest (such as honoraria; educational grants; participation in speakers' bureaus; membership, employment, consultancies, stock ownership, or other equity interest; and expert testimony or patent-licensing arrangements) or non-financial interest (such as personal or professional relationships, affiliations, knowledge, or beliefs) in the subject matter or materials discussed in this paper.

References

1 Makita S, Hong Y, Yamanari M, Yatagai T, Yasuno Y. Optical coherence angiography. Opt Express. 2006 Aug;14(17):7821–40.
2 Jia Y, Tan O, Tokayer J, Potsaid B, Wang Y, Liu JJ, et al. Split-spectrum amplitude-decorrelation angiography with optical coherence tomography. Opt Express. 2012 Feb;20(4):4710–25.
3 Shin JW, Sung KR, Lee JY, Kwon J, Seong M. Optical coherence tomography angiography vessel density mapping at various retinal layers in healthy and normal tension glaucoma eyes. Graefes Arch Clin Exp Ophthalmol. 2017 Jun;255(6):1193–202.
4 Park JJ, Soetikno BT, Fawzi AA. Characterization of the middle capillary plexus using optical coherence tomography angiography in healthy and diabetic eyes. Retina. 2016 Nov;36(11):2039–50.
5 Campbell J, Zhang M, Hwang T, Bailey S, Wilson D, Jia Y, et al. Detailed vascular anatomy of the human retina by projection-resolved optical coherence tomography angiography. Sci Rep. 2017 Feb;7:42201.
6 Munk MR, Giannakaki-Zimmermann H, Berger L, Huf W, Ebneter A, Wolf S, et a. OCT-angiography: a qualitative and quantitative comparison of 4 OCT-A devices. PLoS One. 2017 May;12(5):e0177059.
7 Arya M, Rebhun CB, Alibhai AY, Chen X, Moreira-Neto C, Baumal CR, et al. Parafoveal Retinal Vessel Density Assessment by Optical Coherence Tomography Angiography in Healthy Eyes. Ophthalmic Surg Lasers Imaging Retina. 2018 Oct;49(10):S5–17.
8 Lupidi M, Coscas F, Cagini C, Fiore T, Spaccini E, Fruttini D, et al. Automated quantitative analysis of retinal microvasculature in normal eyes on optical coherence tomography angiography. Am J Ophthalmol. 2016 Sep;169:9–23.
9 Rabiolo A, Gelormini F, Sacconi R, Cicinelli MV, Triolo G, Bettin P, et al. Comparison of methods to quantify macular and peripapillary vessel density in optical coherence tomography angiography. PLoS One. 2018 Oct;13(10):e0205773.
10 Frangi AF, Niessen WJ, Vincken KL, Viergever MA. Multiscale vessel enhancement filtering. Berlin: Springer Berlin Heidelberg; 1998. pp. 130–7.
11 Otsu N. A threshold selection method from gray-level histograms. IEEE Trans Syst Man Cybern. 1979;9(1):62–6.
12 Giavarina D. Understanding Bland Altman analysis. Biochem Med (Zagreb). 2015 Jun;25(2):141–51.
13 de Carlo TE, Chin AT, Bonini Filho MA, Adhi M, Branchini L, Salz DA, et al. Detection of microvascular changes in eyes of patients with diabetes but not clinical diabetic retinopathy using optical coherence tomography angiography. Retina. 2015 Nov;35(11):2364–70.
14 Chalam KV, Sambhav K. Optical coherence tomography angiography in retinal diseases. J Ophthalmic Vis Res. 2016 Jan-Mar;11(1):84–92.
15 Wylęgała A. Principles of OCTA and Applications in Clinical Neurology. Curr Neurol Neurosci Rep. 2018 Oct;18(12):96.
16 Takase N, Nozaki M, Kato A, Ozeki H, Yoshida M, Ogura Y. Enlargement of foveal avascular zone in diabetic eyes evaluated by en face optical coherence tomography angiography. Retina. 2015 Nov;35(11):2377–83.
17 Choi J, Kwon J, Shin JW, Lee J, Lee S, Kook MS. Quantitative optical coherence tomography angiography of macular vascular structure and foveal avascular zone in glaucoma. PLoS One. 2017 Sep;12(9):e0184948.
18 Dimitrova G, Chihara E, Takahashi H, Amano H, Okazaki K. Quantitative retinal optical coherence tomography angiography in patients with diabetes without diabetic retinopathy. Invest Ophthalmol Vis Sci. 2017 Jan;58(1):190–6.
19 Jia Y, Bailey ST, Wilson DJ, Tan O, Klein ML, Flaxel CJ, et al. Quantitative optical coherence tomography angiography of choroidal neovascularization in age-related macular degeneration. Ophthalmology. 2014 Jul;121(7):1435–44.
20 Jia Y, Wei E, Wang X, Zhang X, Morrison JC, Parikh M, et al. Optical coherence tomography angiography of optic disc perfusion in glaucoma. Ophthalmology. 2014 Jul;121(7):1322–32.
21 Hwang TS, Zhang M, Bhavsar K, Zhang X, Campbell JP, Lin P, et al. Visualization of 3 distinct retinal plexuses by projection-resolved optical coherence tomography angiography in diabetic retinopathy. JAMA Ophthalmol. 2016 Dec;134(12):1411–9.